

On the density and temperature of neutron-rich systems at the energy of vanishing flow in heavy-ion collisions

Sakshi Gautam ¹

Department of Physics, Panjab University, Chandigarh -160 014, India.

We study nuclear dynamics at the the energy of vanishing flow for neutron-rich systems. In particular, we shall study the collision rate, density and temperature reached in a heavy-ion reaction with neutron-rich systems. We shall also study the mass dependence of these quantities. Our results indicate nearly mass independent nature for the density reached whereas a significant mass dependence exists for the temperature of neutron-rich systems.

arXiv:1105.0526v1 [nucl-th] 3 May 2011

¹Email: sakshigautm@gmail.com

1 Introduction

The collective transverse in-plane flow has been used extensively over the past three decades to study the properties of hot and dense nuclear matter., i.e., the nuclear matter equation of state (EOS) and in-medium nucleon-nucleon cross section [1]. It has been reported to be highly sensitive to the above mentioned properties and also to the entrance channel parameters like incident energy, colliding geometry and system size [2–6]. The energy dependence of flow led to its disappearance at a particular incident energy called energy of vanishing flow (EVF) or balance energy (E_{bal}) [7]. A large number of theoretical studies have been carried out in the past studying the sensitivity of E_{bal} to the system size and colliding geometry [8–10].

Role of isospin degree of freedom in collective transverse in-plane flow and its disappearance has also been a matter of great interest for the past decade [11, 12]. Isospin degree of freedom plays its role in determining the nuclear equation of state of asymmetric nuclear matter. The availability of radioactive ion beams (RIBs) [13, 14] around the world helps in carrying out the studies on the matter lying far away from the stability line. A number of studies have been carried out in the recent past to see the role of isospin degree of freedom in collective flow and its disappearance [11, 12, 15]. In Ref. [16] author and others studied the isospin effects in E_{bal} at all the colliding geometries. A very few studies have been carried out to study other related phenomena at E_{bal} of the neutron-rich systems. In Ref. [17] Sood and Puri have presented a complete study of the nuclear dynamics at E_{bal} for stable systems. The study includes participant-spectator matter, density and temperature reached in a heavy-ion reaction at E_{bal} . Motivated by this, author and others presented a study of participant-spectator matter of neutron-rich systems at E_{bal} in Ref. [18]. The study revealed a similar behaviour of participant-spectator matter for neutron-rich systems as for the stable systems. Another important quantity which reflects the dynamics in a heavy-ion collision is the density and temperature reached in a reaction. In the present paper, we study the density and temperature reached in heavy-ion reactions of neutron-rich matter at E_{bal} . We also aim to see the role of isospin degree of freedom in the density and temperature reached in the reactions of neutron-rich systems and to see if the behaviour of these properties at balance energy differs from that for systems lie close to the stability line.

The present study is carried out within the framework of isospin-dependent quantum

molecular dynamics (IQMD) model [19]. Section 2 describes the model in brief. Section 3 explains the results and gives our discussion, and Sec. 4 summarizes the results.

2 The model

The IQMD model [19] which is the extension of quantum molecular dynamics (QMD) [20] model treats different charge states of nucleons, deltas, and pions explicitly, as inherited from the Vlasov-Uehling-Uhlenbeck (VUU) model. The IQMD model has been used successfully for the analysis of a large number of observables from low to relativistic energies. Puri and coworkers have demonstrated that QMD, IQMD carries essential physics needed to demonstrate the various phenomena such as collective flow, multifragmentation and particle production [21, 22]. The isospin degree of freedom enters into the calculations via symmetry potential, cross sections, and Coulomb interaction.

In this model, baryons are represented by Gaussian-shaped density distributions

$$f_i(\vec{r}, \vec{p}, t) = \frac{1}{\pi^2 \hbar^2} \exp(-[\vec{r} - \vec{r}_i(t)]^2 \frac{1}{2L}) \times \exp(-[\vec{p} - \vec{p}_i(t)]^2 \frac{2L}{\hbar^2}) \quad (1)$$

Nucleons are initialized in a sphere with radius $R = 1.12 A^{1/3}$ fm, in accordance with liquid-drop model. Each nucleon occupies a volume of h^3 , so that phase space is uniformly filled. The initial momenta are randomly chosen between 0 and Fermi momentum (\vec{p}_F). The nucleons of the target and projectile interact by two- and three-body Skyrme forces, Yukawa potential, and Coulomb interactions. In addition to the use of explicit charge states of all baryons and mesons, a symmetry potential between protons and neutrons corresponding to the Bethe-Weizsäcker mass formula has been included. The hadrons propagate using Hamilton equations of motion:

$$\frac{d\vec{r}_i}{dt} = \frac{d\langle H \rangle}{d\vec{p}_i}; \quad \frac{d\vec{p}_i}{dt} = -\frac{d\langle H \rangle}{d\vec{r}_i} \quad (2)$$

with

$$\begin{aligned} \langle H \rangle &= \langle T \rangle + \langle V \rangle \\ &= \sum_i \frac{p_i^2}{2m_i} + \sum_i \sum_{j>i} \int f_i(\vec{r}, \vec{p}, t) V^{ij}(\vec{r}', \vec{r}) \\ &\quad \times f_j(\vec{r}', \vec{p}', t) d\vec{r}' d\vec{r}' d\vec{p}' d\vec{p}'. \end{aligned} \quad (3)$$

The baryon potential V^{ij} in the above relation, reads as

$$\begin{aligned}
V^{ij}(\vec{r}' - \vec{r}) &= V_{\text{Skyrme}}^{ij} + V_{\text{Yukawa}}^{ij} + V_{\text{Coul}}^{ij} + V_{\text{sym}}^{ij} \\
&= [t_1\delta(\vec{r}' - \vec{r}) + t_2\delta(\vec{r}' - \vec{r})\rho^{\gamma-1}(\frac{\vec{r}' + \vec{r}}{2})] \\
&\quad + t_3\frac{\exp(-|\vec{r}' - \vec{r}|/\mu)}{(|\vec{r}' - \vec{r}|/\mu)} + \frac{Z_i Z_j e^2}{|\vec{r}' - \vec{r}|} \\
&\quad + t_4\frac{1}{\varrho_0}T_{3i}T_{3j}\delta(\vec{r}'_i - \vec{r}'_j). \tag{4}
\end{aligned}$$

Here Z_i and Z_j denote the charges of i th and j th baryon, and T_{3i} and T_{3j} are their respective T_3 components (i.e., $1/2$ for protons and $-1/2$ for neutrons). The parameters μ and t_1, \dots, t_4 are adjusted to the real part of the nucleonic optical potential. For the density dependence of the nucleon optical potential, standard Skyrme type parametrization is employed. We use a soft equation of state along with the standard isospin- and energy-dependent cross section reduced by 20%, i.e. $\sigma = 0.8 \sigma_{nn}^{free}$. In a recent study, Gautam *et al.* [15] has confronted the theoretical calculations of IQMD with the data of $^{58}\text{Ni} + ^{58}\text{Ni}$ and $^{58}\text{Fe} + ^{58}\text{Fe}$ [11]. The results with the soft EOS (along with the momentum-dependent interactions) and above choice of cross section are in good agreement with the data at all colliding geometries. The details about the elastic and inelastic cross sections for proton-proton and proton-neutron collisions can be found in [19, 23]. The cross sections for neutron-neutron collisions are assumed to be equal to the proton-proton cross sections. Two particles collide if their minimum distance d fulfills

$$d \leq d_0 = \sqrt{\frac{\sigma_{tot}}{\pi}}, \sigma_{tot} = \sigma(\sqrt{s}, type), \tag{5}$$

where 'type' denotes the ingoing collision partners (N-N....). Explicit Pauli blocking is also included; i.e. Pauli blocking of the neutrons and protons is treated separately. We assume that each nucleon occupies a sphere in coordinate and momentum space. This trick yields the same Pauli blocking ratio as an exact calculation of the overlap of the Gaussians will yield. We calculate the fractions P_1 and P_2 of final phase space for each of the two scattering partners that are already occupied by other nucleons with the same isospin as that of scattered ones. The collision is blocked with the probability

$$P_{block} = 1 - [1 - \min(P_1, 1)][1 - \min(P_2, 1)], \tag{6}$$

and, correspondingly is allowed with the probability $1 - P_{block}$. For a nucleus in its ground state, we obtain an averaged blocking probability $\langle P_{block} \rangle = 0.96$. Whenever an attempted collision is blocked, the scattering partners maintain the original momenta prior to scattering.

3 Results and discussion

We simulate the reactions of Ca+Ca, Ni+Ni, Zr+Zr, Sn+Sn, and Xe+Xe series having $N/Z = 1.0, 1.6$ and 2.0 . In particular, we simulate the reactions of $^{40}\text{Ca}+^{40}\text{Ca}$ (105), $^{52}\text{Ca}+^{52}\text{Ca}$ (85), $^{60}\text{Ca}+^{60}\text{Ca}$ (73); $^{58}\text{Ni}+^{58}\text{Ni}$ (98), $^{72}\text{Ni}+^{72}\text{Ni}$ (82), $^{84}\text{Ni}+^{84}\text{Ni}$ (72); $^{81}\text{Zr}+^{81}\text{Zr}$ (86), $^{104}\text{Zr}+^{104}\text{Zr}$ (74), $^{120}\text{Zr}+^{120}\text{Zr}$ (67); $^{100}\text{Sn}+^{100}\text{Sn}$ (82), $^{129}\text{Sn}+^{129}\text{Sn}$ (72), $^{150}\text{Sn}+^{150}\text{Sn}$ (64) and $^{110}\text{Xe}+^{110}\text{Xe}$ (76), $^{140}\text{Xe}+^{140}\text{Xe}$ (68) and $^{162}\text{Xe}+^{162}\text{Xe}$ (61) at an impact parameter of $b/b_{\max} = 0.2-0.4$ and at the incident energies equal to balance energy. The values in the brackets represent the balance energies for the systems. The reactions are followed till the transverse in-plane flow saturates. It is worth mentioning here that the saturation time varies with the mass of the system. It has been shown in Ref. [24] that the transverse in-plane flow in lighter colliding nuclei saturates earlier compared to heavy colliding nuclei. Saturation time is about 100 (150 fm/c) in lighter (heavy) colliding nuclei in the present energy domain. We use the quantity "directed transverse momentum $\langle p_x^{dir} \rangle$ " to define the nuclear transverse in-plane flow, which is defined as [19, 20, 25]

$$\langle p_x^{dir} \rangle = \frac{1}{A} \sum_{i=1}^A \text{sign}\{y(i)\} p_x(i), \quad (7)$$

where $y(i)$ and $p_x(i)$ are, respectively, the rapidity (calculated in the center of mass system) and the momentum of the i^{th} particle. The rapidity is defined as

$$Y(i) = \frac{1}{2} \ln \frac{\vec{E}(i) + \vec{p}_z(i)}{\vec{E}(i) - \vec{p}_z(i)}, \quad (8)$$

where $\vec{E}(i)$ and $\vec{p}_z(i)$ are, respectively, the energy and longitudinal momentum of the i^{th} particle. In this definition, all the rapidity bins are taken into account.

In fig. 1(a), we display the time evolution of average density (ρ^{avg}/ρ_0) whereas fig. 1(b) displays the time evolution of maximum density (ρ^{max}/ρ_0) for the systems having $N/Z = 1.0$, i.e, we display the reactions of $^{40}\text{Ca}+^{40}\text{Ca}$, $^{58}\text{Ni}+^{58}\text{Ni}$, $^{81}\text{Zr}+^{81}\text{Zr}$, $^{100}\text{Sn}+^{100}\text{Sn}$,

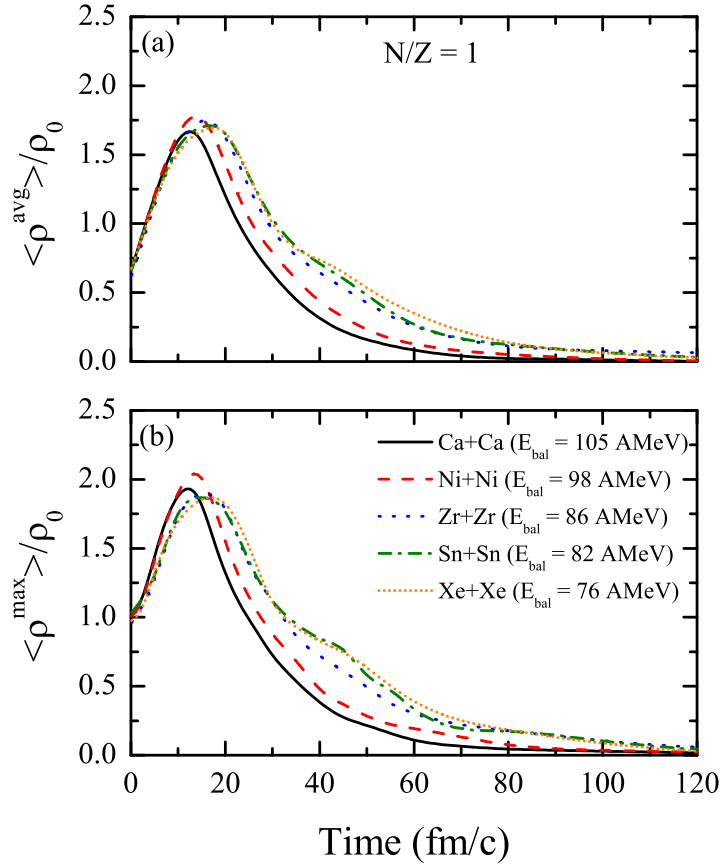


Figure 1: (Color online) The time evolution of spectator matter (left panels) and participant matter (right panels) for systems having $N/Z = 1.0, 1.6$ and 2.0 . Lines are explained in the text.

and $^{110}\text{Xe}+^{110}\text{Xe}$ at energy equal to balance energy. Lines represent the different systems. Solid, dashed, dotted, dash-dotted, and short dotted lines represent the reactions of Ca+Ca, Ni+Ni, Zr+Zr, Sn+Sn, and Xe+Xe, respectively. From figure, we find that maximal value of ρ^{avg}/ρ_0 is higher for lighter systems as compared to the heavier ones. Moreover, the density profile is more extended in heavier systems indicating that the reaction finishes later in heavier systems. This is because of the fact that the heavier reaction occurs at low incident energy. Also the ρ^{avg}/ρ_0 and ρ^{max}/ρ_0 are nearly same for heavier systems but differ for lighter systems as in Ref. Further, the maximum and average densities are comparable for medium and heavy mass systems indicating that the dense matter is formed widely and uniformly in the central zone of the reaction. On the other hand, the substantial difference in two densities for the lighter colliding nuclei has been explained in Ref. [17] and indicates the non-homogeneous nature of dense matter. It

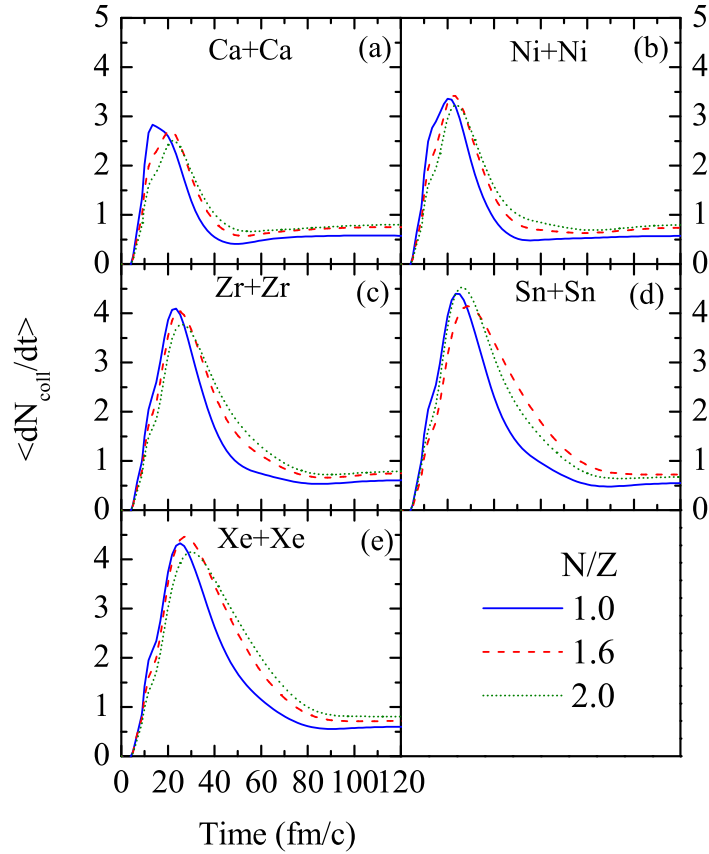


Figure 2: (Color online) The N/Z dependence of participant and spectator matter. Symbols are explained in the text.

is worth mentioning that collective flow saturates at higher densities whereas multifragmentation occurs at sub-density zone. Other phenomena such as fusion-fission are very low density phenomena [26].

The quantity which reflects the density achieved in a reaction is the collision rate. In fig. 2, we display the time evolution of the collision rate for various systems having $N/Z = 1.0, 1.6$ and 2.0 . Solid, dashed and dotted lines corresponds to systems having $N/Z = 1.0, 1.6$ and 2.0 , respectively. From figure, we see that collision rate first increases with time, reaches maximum at around 20-40 fm/c (which is the high dense phase of the reaction) and then finally decreases and becomes constant at around 80 fm/c. We also find that

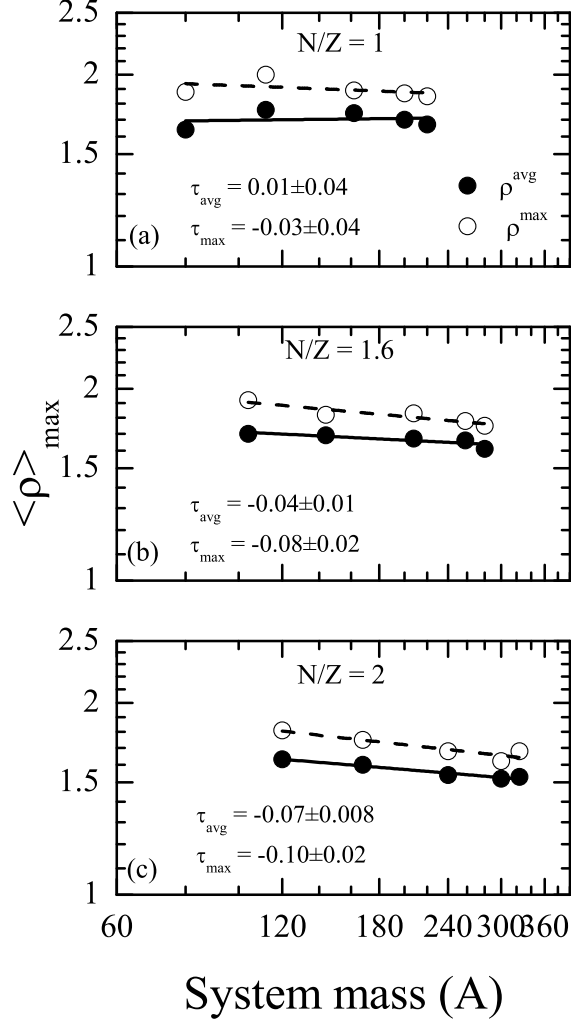


Figure 3: The system size dependence of participant and spectator matter for different N/Z ratios. Various symbols are explained in the text.

the maximum value of the collision rate also increases with the system mass. Moreover, the effect of N/Z ratio on the collision rate is very less.

In fig. 3 we display the system size dependence of maximal value of the maximum (ρ^{max}) and average density (ρ^{avg}) for the systems having N/Z = 1.0, 1.6 and 2.0. We see that the maximal value of ρ^{max} and ρ^{avg} follows a power law behaviour proportional to

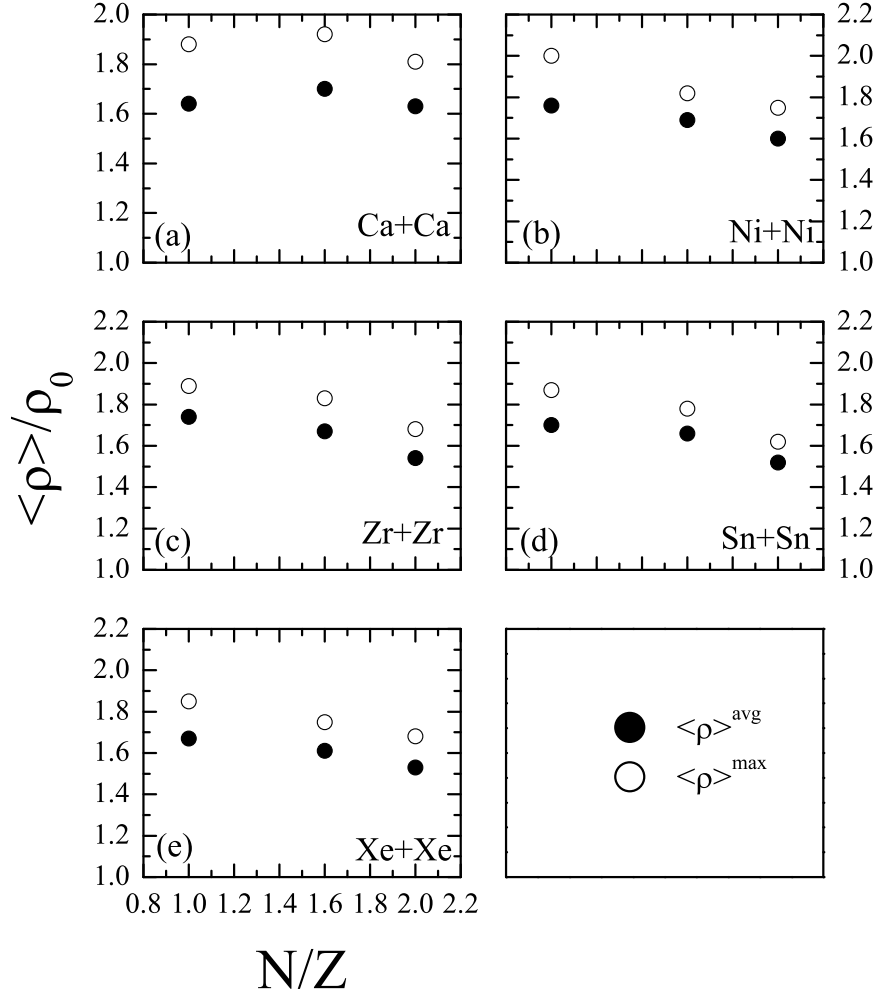


Figure 4: The N/Z dependence of participant and spectator matter. Symbols are explained in the text.

A^τ . The power law factor is 0.01 ± 0.04 (-0.03 ± 0.04), -0.04 ± 0.01 (-0.08 ± 0.02), and -0.07 ± 0.008 (-0.10 ± 0.02) for ρ^{avg} (ρ^{max}) for systems with N/Z = 1.0, 1.6 and 2.0, respectively. It shows that the dependence of maximal value of ρ^{avg} and ρ^{max} is very weak on the system size for all the N/Z ratios. This was also predicted in Ref.citesood2 for stable systems.

In fig. 4 we display the N/Z dependence of maximal value of ρ^{avg} and ρ^{max} . Solid

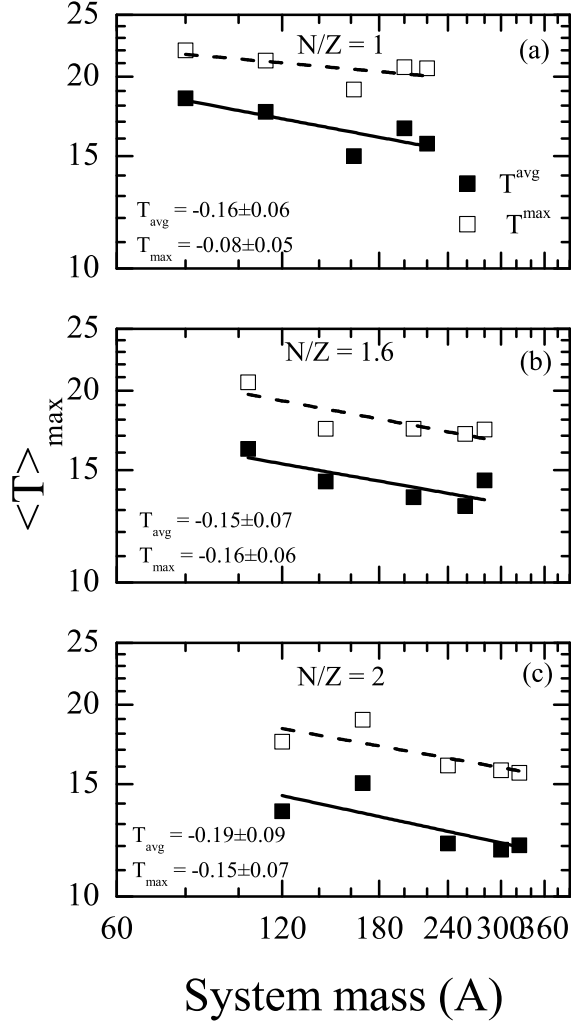


Figure 5: The system size dependence of anisotropy ratio for various N/Z ratios.

(open) symbols display the results for ρ^{avg} (ρ^{max}). From figure we see that both ρ^{avg} and ρ^{max} decreases slightly with N/Z of the system for all the system masses. A slight exception to this is there for the lighter mass of Ca+Ca.

The another associated quantity linked with the dense matter is the temperature. In principle, a true temperature can be defined only for a thermalized and equilibrated matter. Since in heavy-ion collisions the matter is non-equilibrated, one can not talk of “temperature”. One can, however, look in terms of the local environment only. In our present case, we follow the description of the temperature given in Refs. [27,28]. In the present case, extraction of the temperature T is based on the local density approximation,

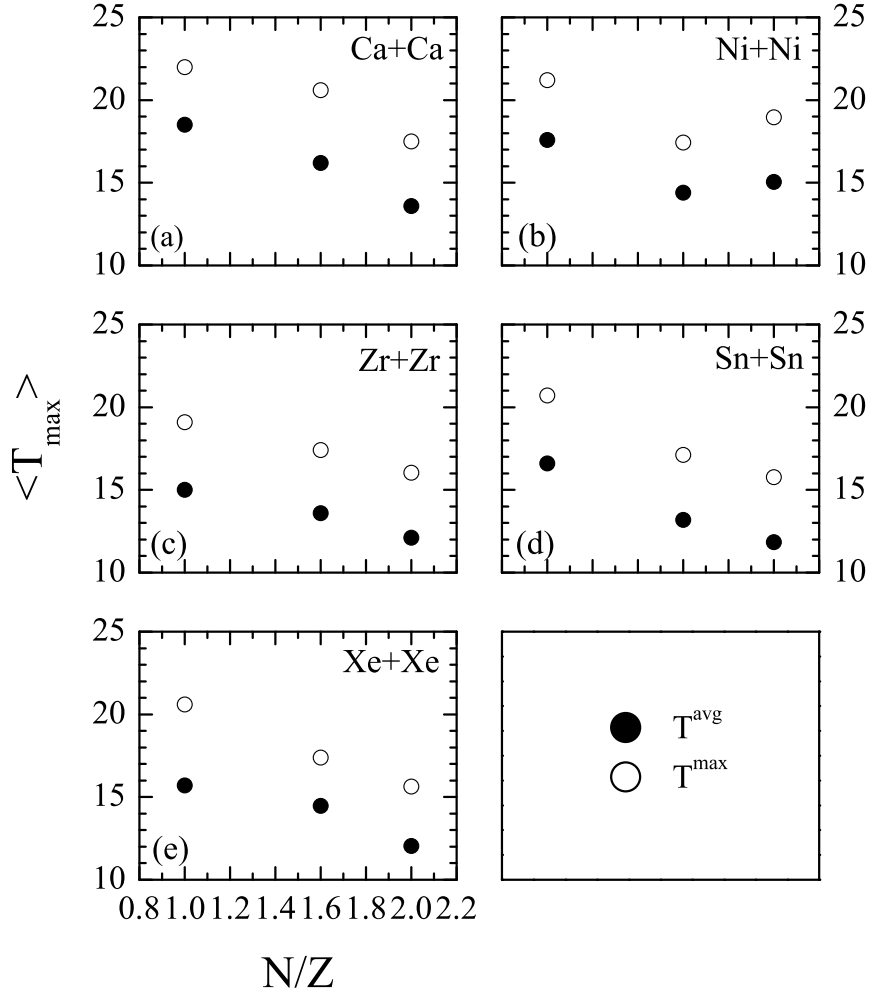


Figure 6: The system size dependence of anisotropy ratio for various N/Z ratios.

i.e., one deduces the temperature in a volume element surrounding the position of each particle at a given time step [27, 28]. Here, we postulate that each local volume element of nuclear matter in coordinate space and time has some “temperature” defined by the diffused edge of the deformed Fermi distribution consisting of two colliding Fermi spheres, which is typical for a nonequilibrium momentum distribution in heavy-ion collisions.

In this formalism (dubbed the hot Thomas-Fermi approach [27]), one determines extensive quantities like the density and kinetic energy as well as entropy with the help of momentum distributions at a given temperature. Using this formalism, we also extracted the average and maximum temperature within a central sphere of 2 fm radius as described

in the case of density.

In fig. 5 we display the maximal value of $\langle T^{avg} \rangle$ and $\langle T^{max} \rangle$ as a function of the composite mass of the system. From figure, we see that $\langle T^{avg} \rangle$ and $\langle T^{max} \rangle$ follows a power law behaviour with system mass for all the N/Z ratios. The power law factor is -0.16 ± 0.06 (-0.08 ± 0.05), -0.15 ± 0.07 (-0.16 ± 0.06), and -0.19 ± 0.09 (-0.15 ± 0.07) for $\langle T^{avg} \rangle$ ($\langle T^{max} \rangle$) for systems having N/Z = 1.0, 1.6 and 2.0, respectively. Similar power law behaviour was also predicted in Ref. [17] for stable systems (N/Z \simeq 1). This system size dependence of temperature is sharp in contrast with the density. This is because of the fact that the temperature depends on the kinetic energy of the system.

In fig. 6 we display the N/Z dependence of maximal value of $\langle T^{avg} \rangle$ and $\langle T^{max} \rangle$ for various system masses. Solid (open) symbols represent the maximal value of $\langle T^{avg} \rangle$ ($\langle T^{max} \rangle$). From figure, we see that for all the system masses, $\langle T^{avg} \rangle$ and $\langle T^{max} \rangle$ decreases with N/Z of the system.

4 Summary

We studied the collision rate, density and temperature reached in reactions of neutron-rich systems at energy of vanishing flow. Our results pointed the similar behaviour for neutron-rich systems as for the stable systems. We also investigated the mass dependence of these quantities. We found a very weak mass dependence of the density although the temperature follows a significant mass dependence.

This work has been supported by a grant from Centre of Scientific and Industrial Research (CSIR), Govt. of India. Author is thankful to Profs. J. Aichelin and R. K. Puri for enlightening discussions on the present work.

References

- [1] W. Scheid, H. Müller and W. Greiner, Phys. Rev. Lett. **32**, 741 (1974); H. A. Gustafsson *et al.*, Phys. Rev. Lett. **52**, 1590 (1984).
- [2] C. A. Ogilvie *et al.*, Phys. Rev. C **40**, 2592 (1989); B. Blättel *et al.*, Phys. Rev. C **43**, 2728 (1991).
- [3] A. Andronic *et al.*, Phys. Rev. C **67**, 034907 (2003).

- [4] J. Lukasik *et al.*, Phys. Lett. B **608**, 223 (2005).
- [5] Y. Zhang and Z. Li, Phys. Rev. C **74**, 014602 (2006).
- [6] J. Lukasik and W. Trautmann, arxiv-0708.2821V1 (2008); B. Hong *et al.*, Phys. Rev. C **66**, 034901 (2000).
- [7] D. Krofcheck *et al.*, Phys. Rev. Lett. **63**, 2028 (1989).
- [8] D. J. Majestro *et al.*, Phys. Rev. C **61**, 021602(R) (2000).
- [9] A. D. Sood and R. K. Puri, Eur. Phys. J. A **30**, 571 (2006); *ibid.* Phys. Lett. **B594**, 260 (2004); *ibid.* Phys. Rev. C **73**, 067602 (2006); R. Chugh *et al.*, Phys. Rev. C **82**, 014603 (2010).
- [10] D. J. Majestro, W. Bauer and G. D. Westfall., Phys. Rev. C **62**, 041603(R) (2000).
- [11] R. Pak *et al.*, Phys. Rev. Lett. **78**, 1022 (1997); *ibid.* **78**, 1026 (1997).
- [12] B. A. Li, C. M. Ko, and W. Bauer, Int. J. Mod. Phys. E **7**, 147 (1998); B. A. Li, Z. Ren, C. M. Ko, and S. J. Yennello, Phys. Rev. Lett. **76**, 4492 (1996); C. Liewen, Z. Fengshou, and J. Genming, Phys. Rev. C **58**, 2283 (1998).
- [13] W. Zhan *et al.*, Int. J. Mod. Phys. E **15**, 1941 (2006); see, e.g. <http://www.impcas.ac.cn/zhuye/en/htm/247.htm>.
- [14] Y. Yano, Nucl. Inst. Methods B **261**, 1009 (2007).
- [15] S. Gautam *et al.*, J. Phys G: Nucl. Part. Phys. **37**, 085102 (2010).
- [16] S. Gautam and A. D. Sood, Phys. Rev. C **82**, 014604 (2010); S. Gautam *et al.*, Phys. Rev. C **83**, 014603 (2011).
- [17] A. D. Sood and R. K. Puri, Phys. Rev. C **70**, 034611 (2004).
- [18] S. Gautam and R. K. Puri, Phys. Rev. C (communicated).
- [19] C. Hartnack *et al.*, Eur. Phys. J. A **1**, 151 (1998); C. Hartnack and J. Aichelin, Phys. Rev. C **49**, 2801 (1994); S. Kumar *et al.*, *ibid.* **81**, 014611 (2010); *ibid.* **81**, 014601 (2010); V. Kaur *et al.*, Phys. Lett. **B597**, 612 (2011); S. Gautam *et al.*, Phys. Rev. C **83**, 014603 (2011); *ibid.* C **83**, 034606 (2011).

- [20] J. Aichelin, Phys. Rep. **202**, 233 (1991); Y. K. Vermani *et al.*, J. Phys. G: Nucl. Part. Phys. **36**, 105103 (2009); *ibid.* **37**, 015105 (2010); *ibid.* Eur Phys Lett **85**, 62001 (2010); *ibid.* Phys. Rev. C **79**, 064613 (2009), Nucl. Phys A **847**, 243 (2010).
- [21] J. Dhawan *et al.*, Phys. Rev. C **74**, 057901 (2006); *ibid.* C **74**, 054610 (2006); S. Kumar *et al.*, Phys. Rev. C **58**, 320 (1998); *ibid.* C **57**, 2744 (1998); *ibid.* C **78**, 064602 (2008).
- [22] G. Batko *et al.*, J. Phys. G **20**, 461 (1994); *ibid.* J. Phys. G **22**, 131 (1996); E. Lehmann *et al.*, Prog. Part. Nucl. Phys. **30**, 219 (1993); S. W. Huang *et al.*, *ibid.* **30**, 105 (1993).
- [23] J. Cugnon, T. Mizutani, and J. Vandermeulen, Nucl. Phys. **A352**, 505 (1981).
- [24] A. D. Sood and R. K. Puri , Phys. Rev. C **69**, 054612 (2004).
- [25] E. Lehmann *et al.* , Z. Phys. A **355**, 55 (1996).
- [26] R. K. Puri *et al.*, Eur. Phys. J. **A3**, 277 (1998); *ibid.* **A3**, 103 (1998); *ibid.* J. Phys. G: Nucl. Part. Phys. **18**, 1533 (1997); I. Dutt *et al.*, Phys. Rev. C **81**, 064608 (2010); *ibid.* C **81**, 064609 (2010); *ibid.* C **81**, 047601 (2010); *ibid.* C **81**, 044615 (2010).
- [27] D. T. Khoa *et al.*, Nucl. Phys. **A542**, 671 (1992).
- [28] D. T. Khoa *et al.*, Nucl. Phys. **A548**, 102 (1992); R. K. Puri *et al.*, Nucl. Phys. **A575**, 733 (1994).